SME Annual Meeting
Feb. 27 - Mar. 02, 2022, Salt Lake City, UT

Preprint 22-079

CONCEPTS FOR DEVELOPMENT OF SHUTTLE CAR AUTONOMOUS DOCKING WITH A CONTINUOUS MINER USING 3-D DEPTH CAMERAS

S. Miller, Univ. of Kentucky, Lexington, KY
J. Sottile, Univ. of Kentucky, Lexington, KY
H.-P. Chiu, SRI International, Princeton, NJ
S. Schafrik, Univ. of Kentucky, Lexington, KY
A. Krasner, SRI International, Princeton, NJ
M. Sizintsev, SRI International, Princeton, NJ
Z. Agioutantis, Univ. of Kentucky, Lexington, KY
A. Rajvanshi, SRI International, Princeton, NJ

ABSTRACT

In recent years, a great deal of effort has been put into automating mining equipment with the goal of improving worker health and safety and increasing mine productivity. Significant progress has been made in automating mining equipment such as load-haul-dumps and drills in underground environments where global positioning systems are unavailable. This paper addresses automating the task of positioning the shuttle-car (SC) under the continuous-miner (CM) coal-discharge conveyor during cutting and loading operations. A stereo depth camera is mounted on the SC. Machine learning based algorithms are applied on the camera's output to identify the CM discharge conveyor and segment the scene into various regions such as roof, ribs, and personnel. This information is used to plan the shuttle car path to the CM discharge conveyor. The approach currently uses a 1/6th scale continuous miner and shuttle car in an appropriately scaled mock mine.

INTRODUCTION

While many mine health and safety improvements have been made in recent decades, the underground coalmine environment still presents numerous health and safety hazards. In particular, the coalmine working section is an extremely hazardous location. In 2017 and 2018, there were 14 fatalities in US underground coalmines. Of these, nine (64%) had the accident classification of *Powered Haulage*. For example, on January 14, 2019, a surveyor in a Kentucky coalmine was struck and killed by a shuttle car tramming to a feeder. The Final Report on this fatality stated that the "*operator's field of vision was greatly reduced due to the size/height of the shuttle car and the low mining height*" [1]. Considering these hazards, as well as those associated with respirable dust (e.g. coal and silica dust), roof and rib falls, fire, etc., removing miners from hazardous locations to safer ones would greatly benefit miners.

The work presented in this paper focuses on development of shuttle car autonomous navigation from the continuous miner change point to the continuous miner, because this is a hazardous location in a coalmine. The continuous miner (CM) operator, helper, and frequently, the section supervisor, are near the CM. Shuttle-car operator visibility is poor, making it difficult to see these personnel. In addition, shuttle car functions are repetitive and monotonous, leading to the potential lack of attention by the operator. The methodology consists of using a 3-D depth camera to identify objects in the camera field of view and subsequently use this information for path planning and navigation to the CM coal discharge conveyor.

MINE ENVIRONMENT

The mine environment developed for this effort consists of a 1/6th scale mockup of a coalmine room and pillar intersection, continuous miner, and shuttle car.

The simulated mine was selected to replicate a small portion of a room and pillar mine having a 2.4 m coal seam and 6.0 m wide crosscuts and entries. This height is larger than most coalmine heights; however, this height was necessary because of the anticipated need for clearance for the depth camera(s) which could not be reduced to 1/6th scale. The constructed portion of mine was one intersection, representing the last open crosscut. An intersection was chosen because it provides the most options for positioning the continuous miner and shuttle car from different perspectives, e.g., the shuttle car approaching the continuous miner from the straight as well as the shuttle car approaching the continuous miner turning left and turning right.

The mine floor was constructed from ½-in. plywood sheets painted flat black, with dado joints (one meter apart) for fastening the ribs to the mine floor. The mine ribs were made of ¼-inch plywood sheets painted black and cut into 0.40 m strips to correspond with the 2.4 m seam height. The mine roof was also made of ¼-in. plywood painted black with dado joints for attaching it to the ribs. Additional pieces of 0.40 x 0.10 cm plywood were used as endcaps to block any ambient light form the laboratory that houses the mock mine. Figure 1 shows the assembled mine floor and ribs (can of spray paint included for scale).

Figure 1. Simulated mine floor and ribs.

A critical piece of the mock mine environment is the continuous miner. Because the methodology uses red-green-blue (RGB) and depth information to produce a target for the shuttle car, the appearance and functionality of the small-scale CM should closely match that of the production machine. This would make the transition form 1/6th scale to full-scale relatively straightforward. Therefore, it was decided that the CM model needed to include the following attributes:

- the same general appearance and proportions as the full-scale continuous miner,
- the ability to tram with independently controlled crawlers (differential steering) to mimic the tramming capability of a production machine, and
- the ability to raise, lower and pivot the coal discharge conveyor.

It was further determined that the coal discharge conveyor did not require a functional coal chain because the camera would take still images of the conveyor and conveyor motion would not be visible. It was also determined that the front (or head) end motion of the continuous miner was not necessary, because this portion of the machine is generally not visible (nor important) from the perspective of the shuttle car.

Two production continuous miners: Caterpillar's CM445 and Joy Global's (Komatsu) 12CM12 were used as the basis of the CM model. Because of the uniqueness of the appearance/geometry of a CM, it was determined that the body would need to be 3D printed to represent accurately the general appearance of the CM.

A remote control (RC) excavator ($1/12^{th}$ scale Earth Digger 4200XL hydraulic excavator) was found to have crawlers of the correct length and height for the $1/6^{th}$ scale continuous miner. The excavator included a radio-controlled hydraulic system, two brushed motors (one mounted on each crawler assembly) for tramming, and one large brushless dc motor to swing the upper frame and boom of the excavator.

The correct width for the crawlers was established by connecting them with two pieces of aluminum bar (Figure 2) which served as a base for all the printed pieces of the CM body.

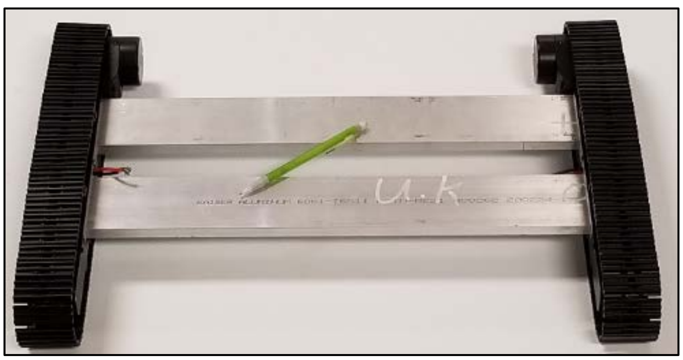

Figure 2. Constructed undercarriage.

The hydraulic system of the RC excavator was modified to raise and lower the discharge conveyor. Two hydraulic cylinders from the excavator were installed in the main body, and connecting rods were attached to the underside of the chain conveyor such that chain conveyor and discharge conveyor would be raised and lowered by the action of the hydraulic cylinder.

To enable the discharge conveyor to pivot, a Savox SB2290SG high-torque servomotor was installed at the pivot point between the coal conveyor and coal discharge conveyor. The servomotor horn was then fastened to the underside of the discharge conveyor, and roller transfer bearings were added to decrease the sliding friction of the discharge conveyor.

The scale-model power supply is a 5000 mAh 11.1 V lithium polymer battery with an XT60 Plug. A custom, eight-channel, 2.4 GHz radio transmitter and corresponding remote-control receiver are used to control the hydraulic valves, the traction motors, and the servomotor.

Autodesk Fusion 360 was used to develop dimensional drawings for 3-D printing the CM body. Approximately 40 individual drawings were developed and exported to the stereo lithography (STL) file format for 3-D printing. The printed parts were then assembled with bolts and threaded inserts to construct the continuous miner body. Figure 3 shows the Autodesk Fusion 360 design of the CM and Figure 4 shows the assembled mockup continuous miner. Figure 5 shows the CM in the mock mine (without the roof).

The shuttle car used in this research (Figure 6) was available from another project, with modifications made to its functionality for this application. Details of the shuttle car construction can be found in [2]; modifications to its control will be discussed in the control section of this paper.

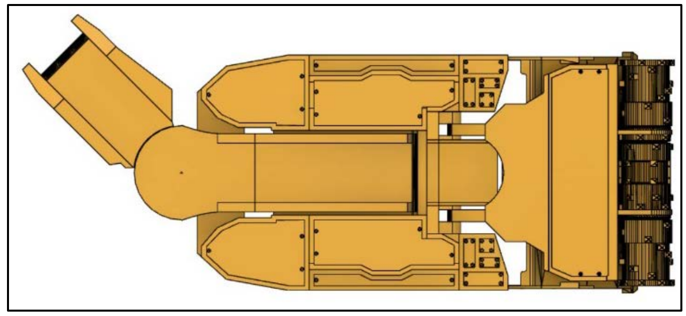

Figure 3. Autodesk Fusion design of 1/6th scale continuous miner.

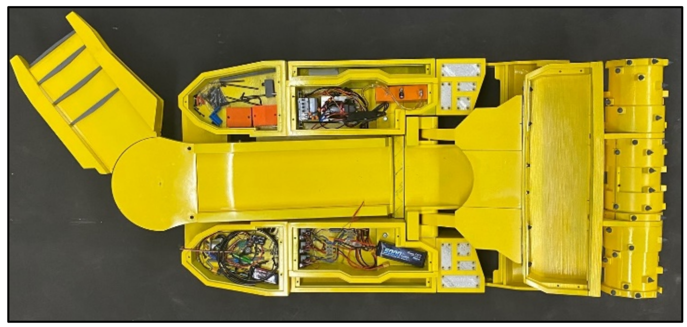

Figure 4. Assembled 1/6th scale continuous miner.

Figure 5. Completed CM model in simulated mine.

SENSORS AND IMAGE ANNOTATION

As mentioned in the Introduction, the approach uses 3D depth cameras and object identification for navigation. The depth camera selected for this research is the Intel RealSense D435i. It was selected because the Intel RealSense camera has three lenses – standard 2D color camera, infrared camera, and infrared laser projector that significantly improves stereo camera ability to tell distance between objects and separate objects from the background. In addition, the Intel RealSense cameras were developed primarily for sensing depth for robots and drones, which matches this application. This camera series also works well in low light. The camera has a wide field of view, which is beneficial for reducing blind spots for collision avoidance. It includes an IMU (inertial measurement unit) for detecting movement and rotation. Another reason for choosing this camera is that the minimum range of the D435i is listed as 0.105 m, which is a good match for the $1/6^{th}$ scale prototype. The RealSense D435i is low-cost and has good SWAP (size, weight, and power) characteristics for the $1/6^{th}$ scale prototype. Finally, several members of the research team have extensive experience with the Intel RealSense D435i camera, and it has performed very well for object recognition and distance measurement.

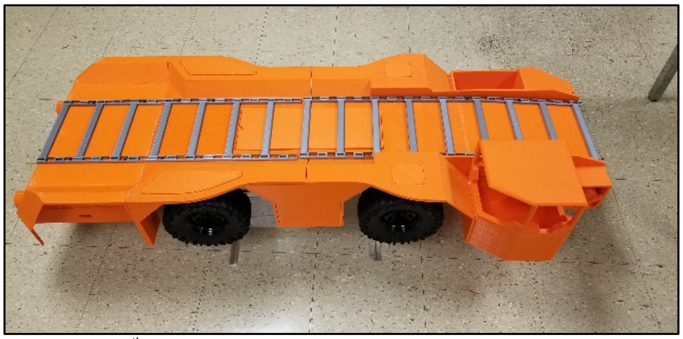

Figure 6. 1/6th scale shuttle car.

Although there exists a large database of images for objects such as people, cars, trucks, traffic signals, and so forth, no such database for coalmine continuous miners was available. Therefore, considerable effort had to be expended in manually annotation images for developing the semantic segmentation step of the autonomous navigation process (described in the next section).

Briefly, image annotation is the process of annotating an image with labels chosen to give the computer-vision model information about what is shown in the image. Details of image annotation will not be included here because there are many excellent sources available that describe the process (e.g., [3]). For this application, image annotation involved manually outlining the CM body and coal discharge conveyor with polygons and labeling each polygon. Over 200 images from various distances and perspectives were annotated. Figure 7 shows an example of one of the annotated images for the continuous miner turning a crosscut to the left.

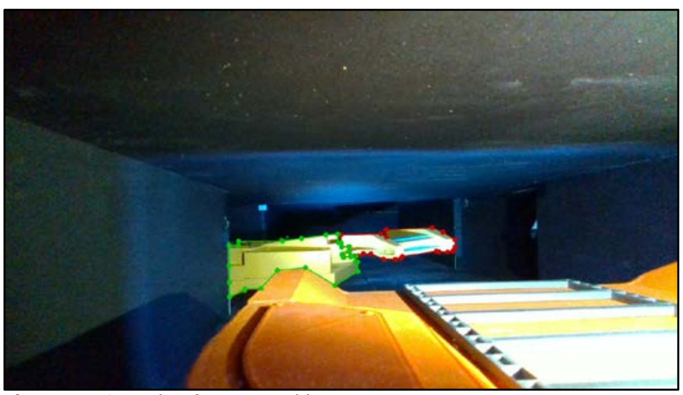

Figure 7. Sample of annotated image.

AUTONOMOUS NAVIGATION METHODOLOGY

The pipeline (Figure 8) retrieves synchronized color and depth images from the camera mounted on the shuttle car and includes the following five processing steps for navigating the shuttle car toward the continuous miner.

1) **Semantic Segmentation:** Segmentation of red-green-blue (RGB) image into various classes
2) **CM Detection:** Detection of the CM in 3D space using RGB and depth data
3) **CM Pose Estimation:** 3D orientation estimation of the CM using depth data within detection
4) **Occupancy Map Construction:** Generation of a discretized 2D environment representation
5) **Path Planning:** Path planning on the generated occupancy map from the SC's current pose to the desired pose (based on the CM's estimated pose).

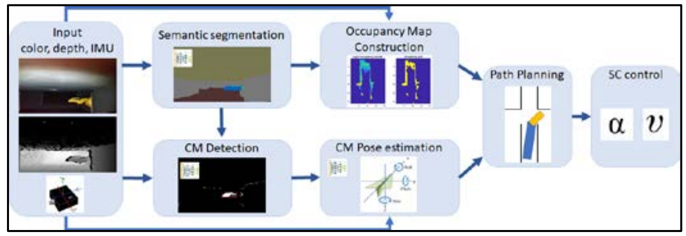

Figure 8. Block diagram of shuttle car autonomous navigation toward the continuous miner.

The path planning output will be fed to the controller driving the shuttle car. These steps will be run in iterations to refine the path as the SC moves towards the CM. Additional details of the pipeline are given below.

Semantic Segmentation and CM Detection: A customized segmentation neural network [4] is applied that is designed to automatically label each imaged pixel into different classes (floor, ceiling, ribs, people, and many object classes) in dark environments, such as mines. The team also trained a separate state-of-the-art RedNet architecture [5] for CM detection from the scene, using synthetic images from simulation using CAD model of the CM discharge conveyor. This network takes RGB and depth images, and produces two-class segmentation masks, where each pixel value is indicative of how likely or not it belongs to the CM. The plan for the future is to combine these two steps into one single neural network for more efficient use of computational resources.

CM Pose Estimation: Once the CM has been detected from the sensory data, another trained RedNet architecture is used to operate on only the depth image of the detected CM region for pose estimation. The pose output is essentially two angle numbers for yaw (a.k.a. heading) and pitch angles (angles in horizontal and vertical planes). The network does not attempt to estimate the roll of the CM (in-image-plain rotation), because it can be assumed that the CM resides on roughly the same ground plane as the shuttle car, making the roll angle very close to zero.

The CM pose estimation performance has been evaluated on the datasets of the 1/6 lab-scale prototype, which contains hand-labelled annotations for the CM discharge conveyor (as well as the CM body) as ground truth. The mean of the error is close to zero, and the standard deviation is around 1.1 degrees. This demonstrated good performance of the semantic segmentation, CM detection, and CM pose estimation. Figure 9 shows two test examples of CM detection and CM pose estimation (yaw degree).

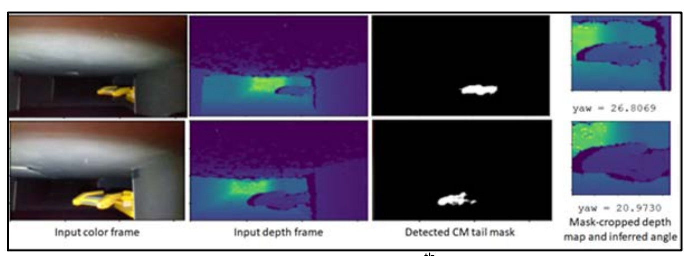

Figure 9. Two examples form the 1/6th scale mock mine and equipment (from left to right): Input RGB image, input depth frame, detected CM mask, correspondent depth map of the detected CM with the yaw angle from the estimated orientation.

Occupancy Map Construction: The ultimate goal of the pipeline is to navigate the SC from its initial pose (x_i, y_i, θ_i) to the final pose (x_f, y_f, θ_f) which is decided based on the estimated pose of the CM. The planned path is also expected to avoid obstacles and follow the SC kinematics and dynamics toward the CM. To develop a path plan, considering obstacles, an Occupancy Map is typically used as a discretized 2D representation of the environment. The dense depth data from the input camera makes it possible to perform 3D reconstruction – project most of the visible 2D imaged points to 3D space. The method starts with identifying the floor points (using the semantic segmentation output) and robustly fitting the 3D plane. This determines the ground plane that gives the frame of reference for the top-down view. Then, the remainder of the points identified as ribs and other objects are projected onto the ground plane. Cells with enough point counts are declared as occupied.

Path Planning: Open Motion Planning Library (OMPL) [6] is used for implementing the motion planner to work on the occupancy grid map generated in the previous step. Two different planners that can be dynamically switched in the navigation process were implemented: (1) transition-based rapidly exploring random tree (T-RRT) and (2) RRT Sharp (RRT$^{\#}$). T-RRT aims to find short, low-cost paths without any optimality guarantees. It is relatively quick compared with other flavors of RRT. On the other hand, RRT$^{\#}$ is a variant of RRT* (RRT* is an optimized version of RRT) with an improved convergence rate. This leads to near optimal solutions, but it could take a large amount of time. Figure 10 shows the results of T-RRT and RRT$^{\#}$ on an occupancy grid map. Note this figure is used to illustrate the differences between the two methods and is not intended to represent the size of the CM and SC in the mine entry.

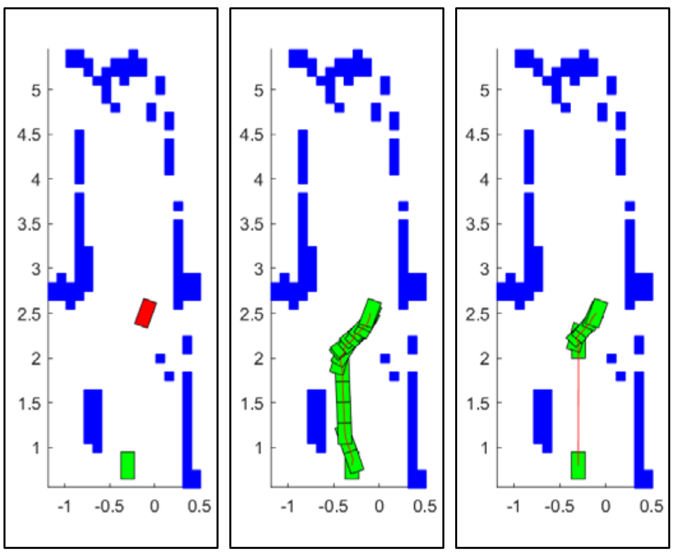

(a) (b) (c)

Figure 10. Planner Results on occupancy map (blue): (a) Start (Green) & Goal (Red), (b) T-RRT, (c) RRT$^{\#}$.

SHUTTLE CAR CONTROL

Shuttle car control is achieved through an Arduino Uno R3, which uses an Atmel ATMega328P, 20 MHz, 8-bit microcontroller with 32 k bytes of flash program memory. This microcontroller includes six analog inputs connected to a 10-bit analog/digital (A/D) converter, and 16 digital pins that can be used as either input or output. Six of these pins provide 8-bit pulse width modulation (PWM) signals. Communication is through UART TTL (5 V) serial communication. A microchip on the Arduino board channels this serial communication over USB and appears as a virtual com port to software on the computer.

As described in [2], the 1/6th scale shuttle car axles are from an off-the-shelf, 1/4 scale, motor-on-axle (MOA) four-wheel drive RC vehicle. Each axle is identical, which permits four-wheel, opposite-direction steering, controlled by two servomotors mounted above each axle. Figure 11 shows the steering servomotors mounted above one of the shuttle car axles.

The steering servomotors are controlled by standard RC PWM signals, in which a pulse is received every 20 ms. A pulse duration of 1500 µs rotates the servo to 90°, its neutral position. Pulse durations of 1000 µs and 2000 µs move the servo to 0° and 180°, respectively. Two PMW channels (one for each axle) are required to control the steering. Although each axle can be controlled independently, each axle is given the identical signal (but opposite direction) to mimic the opposite direction steering of a shuttle car.

Figure 11. 1/6th scale shuttle car steering servomotors.

The shuttle car traction motors are controlled by a 60-V, 2x20 A, brushless dc (BLDC) Motor Controller. This controller can supply two, 12 to 60-V BLDC motors continuously at 20 A, which exceeds the peak operating current and voltage rating of the traction motors selected. This controller was chosen primarily because of the wide range of operating modes available, including pulse (RC radio) mode. The controller also accepts hall sensor or synchronous serial interface (SSI) rotary shaft encoder signals. The controller and traction motors are supplied by a 22.2 V, 5.4 Ah, lithium polymer (LiPo) battery. The controller is programmed to accelerate smoothly, travel a specified distance (dependent on the signal sent to it), and decelerate smoothly. Hall Effect sensors in the traction motors are used as feedback for the (approximate) distance. Figure 12 shows the controller and two traction motors mounted in the shuttle car.

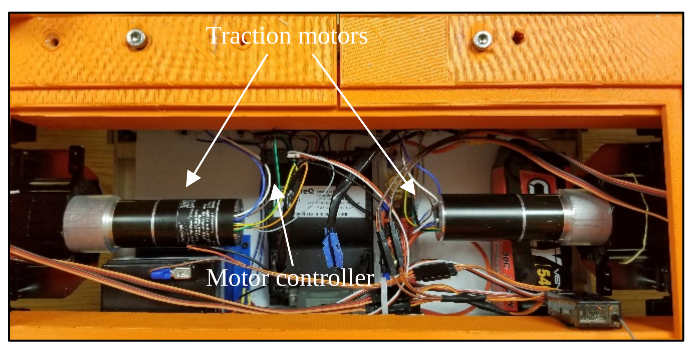

Figure 12. Shuttle car traction motors and controller.

Shuttle car motion is controlled by distance and direction signals generated by the path planner representing waypoints from its current position to its destination. These signals are used to generate PWM signals to achieve the proper steering angle and distance to tram to the next waypoint. It is recognized that this control will have error caused by limitations in precisely controlling the distance and direction, wheel slippage, and so forth. To compensate, the approach is being developed to update trajectory signals frequently to provide course correction as needed. Figure 13 shows a sample of the shuttle car following two consecutive trajectory commands.

CONCLUSION AND FUTURE WORK

Quality training an object recognition algorithm depends on quality input images that are not overly complex and have proper annotation. These algorithms rely on the data set to pick out particular features that are used in the decisions made by the algorithm. Using data collected from the field would not give as useful a data set as can be achieved with a model representation under laboratory conditions.

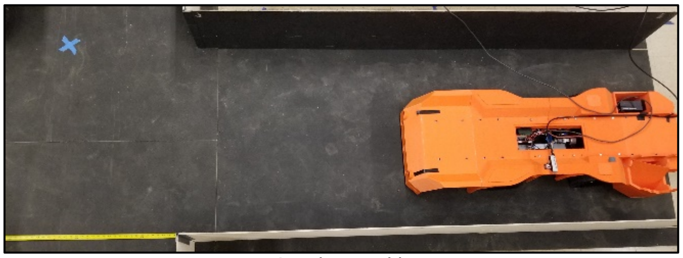

a. Starting position

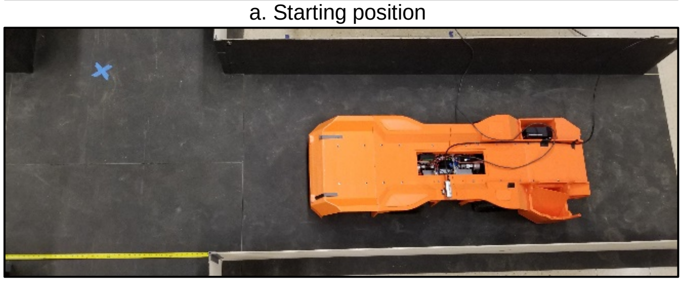

b. Waypoint 1

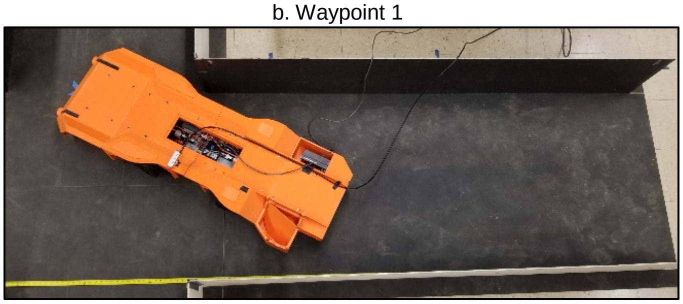

c. Waypoint 2

Figure 13. Shuttle car tramming from starting point (a), to first waypoint (b), to second waypoint (c).

A mock mine and associated equipment have been assembled that create a sufficiently accurate representation of the face area of a coal mine for developing these training sets. Accurate computer recognition is critical in achieving autonomous docking of the shuttle car with the continuous miner using the sensors described in this project. Presented in this work are the individual pieces of the navigation algorithm that are working, using image files. Real time image collection and recognition is being developed and will be discussed in later publications. The algorithm can correctly identify the continuous miner coal-discharge conveyor, estimate its location and pose, construct an occupancy map, and plan a path from the shuttle car current position to the discharge conveyor (with the desired pose). The shuttle car can follow trajectory commands with reasonable accuracy.

Plans for future work include integration of the individual parts into a single program that will permit further evaluation of this approach. Cameras suitable for full-scale image collection will be mounted on a full-scale shuttle car. Images of full-scale mining equipment, in a realistic environment, will be collected and used for modifying the algorithm presented for full-scale testing.

ACKNOWLEDGEMENT

Research reported in this presentation was supported by the National Institute for Occupational Safety and Health (NIOSH) under Contract Number 75D30120C08908. The content is solely the responsibility of the authors and does not necessarily represent the official views of NIOSH.

REFERENCES

1. January 14, 2014 Fatality – Final Report, https://www.msha.gov/data-reports/fatality-reports/2019/january-14-2019-fatality/final-report.

2. V. Androulakis, J. Sottile, S. Schafrik and Z. Agioutantis, "Concepts for Development of Autonomous Coal Mine Shuttle Cars," in *IEEE Transactions on Industry Applications*, vol. 56, no. 3, pp. 3272-3280, May-June 2020, doi: 10.1109/TIA.2020.2972786.

3. Image Annotation 101, Labelbox, https://labelbox.com/image-annotation-overview.

4. Alex Krasner, Mikhail Sizintsev, Abhinav Rajvanshi, Han-Pang Chiu, Niluthpol Mithun, Kevin Kaighn, Philip Miller, Ryan Villamil, Supun Samarasekera, "SIGNAV: Semantically-Informed GPS-Denied Navigation and Mapping in Visually-Degraded Environments", in Winter Conference of Computer Vision (WACV), 2021.

5. Jindong Jiang, Lunan Zheng, Fei Luo, Zhijun Zhang, "RedNet: Residual Encoder-Decoder Network for indoor RGB-D Semantic Segmentation", in Asian Conference on Computer Vision (ACCV), 2020.

6. Open Motion Planning Library (OMPL) https://ompl.kavrakilab.org/.